Published in final edited form as:
Biochemistry. 2010 September 7; 49(35): 7659–7664. doi:10.1021/bi100851c.

Infrared Study of the Folding Mechanism of a Helical Hairpin: Porcine PYY†

Matthias M. Waegele and **Feng Gai***
Department of Chemistry, University of Pennsylvania, Philadelphia, PA 19104

Abstract

The helical hairpin motif plays a key role as a receptor site in DNA-binding and protein-protein interactions. Thus, various helical hairpins have recently been developed to understand the factors that control the DNA- and/or protein-binding affinities of this structural motif and to form synthetic templates for protein and drug design. In addition, several lines of evidence suggest that rapid acquisition of a helical hairpin structure from the unfolded ensemble may guide the rapid formation of helical proteins. Despite its importance as a crucial structural element in protein folding and binding, the folding mechanism of the helical hairpin motif has not been thoroughly studied. Herein, we investigate the structural determinants of the folding kinetics of a naturally occurring helical hairpin (porcine PYY) that is free of disulfide bonds and metal ion-induced cross-links using an infrared temperature-jump technique. It is found that mutations in the turn region predominantly increase the barrier of folding irrespective of the temperature, whereas the effect of mutations that perturb the hydrophobic interactions between the two helices is temperature dependent. At low temperature, deletion of hydrophobic sidechains is found to predominantly affect the unfolding rate, while the opposite is observed at high temperature. These results are interpreted in terms of a folding mechanism in which the turn is formed in the transition state and also based on the assumption that cross-strand hydrophobic contacts exist in the thermally unfolded state of PYY.

Keywords

Porcine PYY; Protein folding; Helical hairpin; Infrared; T-jump

The α-helical hairpin, or helix-turn-helix (HTH) motif, can be regarded as a supersecondary structural element of helical proteins. In many cases, the HTH motif is found to play an important functional role. For example, it is the primary recognition element of a large number of DNA-binding proteins (1,2) and is also involved in protein-protein interactions (2). Therefore, it is not surprising that there has been great interest in designing stable helical hairpins that exhibit high affinity and specificity towards DNA or proteins (3-5). In addition, the HTH motif has been suggested to play an important role in protein folding. Because it encompasses both secondary structural elements and long-range tertiary contacts, a rapidly formed local HTH conformation could serve as a folding nucleus or kernel (6-8), allowing rapid assembly of the entire tertiary structure. For example, Religa *et al.* have shown that the fast phase in the folding kinetics of Engrailed homeodomain (EnHD) arises from the formation of a folding kernel consisting of helices 2 and 3 of the protein (9).

†Supported by the NIH (GM-065978 and RR-01348).

*To whom correspondence should be addressed; gai@sas.upenn.edu; Phone: 215-573-6256; Fax: 215-573-2112.

Because of the structural and functional roles of the HTH motif, the structural determinants and folding/unfolding thermodynamics of various helical hairpins have been extensively studied in the past few years (5,10-12). Though these equilibrium studies provided valuable insights into the factors that control the thermal stability of the HTH motif, they revealed little information on how folding and unfolding actually take place. As a result, our current understanding of the folding mechanism of the HTH motif is mainly based on the kinetic study of a cross-linked α-helical hairpin, Z34C (13), whose termini are covalently connected via a disulfide bond that is introduced to stabilize the folded structure (3). While Z34C is a useful template for protein- and drug-designs (3), it may not be a good model system for understanding the mechanism of α-helical hairpin formation as the disulfide constraint artificially limits the accessible conformational space of the unfolded state ensemble.

To provide further insight into the folding mechanism of the HTH motif, herein we study the folding dynamics of a monomeric, naturally occurring helical hairpin (porcine PYY; sequence: YPAKP-EAPGE-DASPE-ELSRY-YASLR-HYLNL-VTRQR-Y-NH_2) by means of temperature-jump infrared (*T*-jump IR) spectroscopy (14) in conjunction with site-directed mutagenesis (15). As shown (Figure 1), porcine PYY (referred to hereafter as PYY) is free of disulfide bonds and assumes a structure known as the PP-fold in which an N-terminal type II polyproline (PPII) helix folds onto a C-terminal α-helix to form a stable, well defined hydrophobic cluster between the interfaces of the two helices (11,16,17). To dissect the kinetic roles of the two most important structural elements in the PP-fold, i.e., the hydrophobic cluster and the turn, we studied the folding-unfolding kinetics of two sets of PYY mutants. The first set of mutants, A7Y, Y21A, and Y27A, involves residues that contribute to the hydrophobic interactions between the two helices. The second set of mutants, S13A and P14A, targets residues in the turn region of the peptide. Our results support the notion that the turn sequence has a strong influence on the folding rate of hairpin structures (13,18,19) and that the turn sequence in wild-type PYY is highly optimized for folding, whereas the kinetic effect of mutations in the hydrophobic cluster is more complicated.

Materials and Methods

Materials

All materials were used as received. D_2O (D, 99.96%) was purchased from Cambridge Isotope Laboratories (Andover, MA). Amino acids for peptide synthesis were obtained from Advanced ChemTech (Louisville, KY).

Peptide Sample Preparation

The peptides were synthesized using standard flouren-9-ylmethoxycarbonyl (Fmoc)-chemistry on a PS3 peptide synthesizer from Protein Technologies, (Tucson, AZ) and were purified by reversed-phase HPLC (Agilent Technologies, Santa Clara, CA). The mass of each peptide was verified by matrix-assisted laser desorption ionization mass spectrometry (Voyager-DE RP, Applied Biosystems, Foster City, CA). Following purification, the peptide solutions were lyophilized, dissolved in D_2O and titrated to pH* 5.2 ± 0.1 (pH meter reading) with a solution of sodium hydroxide in D_2O. Another round of lyophilization in D_2O ensured complete removal of H_2O. Peptide sample used in spectroscopic measurements were prepared by dissolving an appropriate amount of lyophilized peptide solid in 20 mM D_2O 2-(N-morpholino)ethanesulfonic acid (MES) buffer (pH* 5.2). For circular dichroism (CD) measurements, the peptide concentration was about 40 μM, determined optically using the absorbance of tyrosine at 280 nm and an extinction coefficient of 1492 $cm^{-1}M^{-1}$. For IR measurements, the peptide concentration was in the range of 1 – 4 mM.

CD Measurement and Analysis

CD data were collected on an Aviv Model 410 instrument (Aviv Biomedical, Lakewood, NJ) using a 1 mm cuvette. For thermal unfolding measurements, the CD signal at 222 nm was averaged for 30 s at each temperature. After the highest temperature was reached, the sample was cooled to 25 °C and another full CD spectrum was measured to ensure that unfolding was reversible. The folding-unfolding thermodynamics of PYY and the mutants were determined by globally fitting their CD thermal melting transitions to a two-state model, the detail of the global fitting method has been described previously (20). Briefly, the folded and unfolded CD baselines $\theta_F(T)$ and $\theta_U(T)$ were assumed to be linear functions of temperature, i.e., $\theta_F(T) = m + n \cdot T$, $\theta_U(T) = p + q \cdot T$, and n and q (m and p) were treated as global (local) fitting parameters.

T-jump Relaxation Measurement

The *T*-jump induced relaxation kinetics of PYY and mutants were measured by probing the time-dependent absorbance change of the helical amide I′ band of the peptide at 1631 cm^{-1}. A detailed description of the *T*-jump IR setup can be found elsewhere (21). The only difference is that in the current study the transient IR signals were probed by a tunable quantum cascade laser (Daylight Solutions, Poway, CA). The *T*-jump induced relaxation kinetics of the PYY peptides were found to develop in two distinct phases. The fast kinetic phase is unresolvable due to the 20 ns rise time of the IR detector and is attributed to temperature-induced spectral shift and/or imperfect background subtraction. Thus, only the slow phase, which can be described by a single-exponential function, is considered in the following discussion.

Results and Discussion

The HTH motif has recently attracted much attention due to its DNA- and protein-binding properties (3-5,22) and because of its potential role as a productive (on pathway) intermediate in protein folding (6-8), such as in the case of EnHD (9). Previously, we have shown that the folding mechanism of a cross-linked α-helical hairpin, Z34C, is similar to that of β-hairpins (13), with turn formation playing a dominant role in the folding kinetics of the hairpin. However, because of the disulfide cross-linker it is unclear whether the folding mechanism of Z34C is representative of that of unconstrained α-helical hairpins. Therefore, we extend our study on how α-helical hairpins fold to porcine PYY (11,16,17), a naturally occurring HTH motif free of disulfide bonds.

Folding thermodynamics and kinetics of PYY

As shown (Figure 2), the far-UV CD spectrum of PYY in phosphate buffer (20 mM, pH* 5.2) at 25 °C exhibits the characteristic double minima of α-helices, indicating that it is mostly folded at this temperature. To better quantify the folding/unfolding thermodynamics of PYY and the mutants studied here (see below), we globally analyzed their CD melting curves measured at 222 nm using a global fitting method (see Methods Section for detail). As shown (Figure 3 and Table 1), the thermal melting temperature (T_m) of wild-type PYY thus obtained is 44.0 ± 1.6 °C, which is almost identical to that determined by Zerbe and coworkers using NMR spectroscopy (11).

The conformational relaxation kinetics of PYY in response to a *T*-jump were measured using a time-resolved infrared technique (21) with a probing frequency of 1631 cm^{-1}, where solvated α-helical amides show strong absorbance (23-25). As shown (Figure 4), the *T*-jump induced conformational relaxation of PYY obtained at 32.2 °C, a temperature that is below T_m, occurs on the microsecond timescale, indicating that it folds very rapidly. Indeed, decomposition of the relaxation rate constants into folding and unfolding rate constant based

on a two-state analysis (see Methods section for detail) shows that the folding time constant of PYY is around 3 μs in the temperature range studied (Figure 5). For example, at 30 °C the folding and unfolding rate constants are $(2.8 \pm 0.5\ \mu s)^{-1}$ and $(7.1 \pm 1.3\ \mu s)^{-1}$, respectively (Table 2). Interestingly, the α-helical hairpin Z34C, whose folded structure is stabilized by a disulfide bond that links the N- and C-termini of the peptide, folds with a similar rate (13). Taken together, these results thus corroborate our previous notion that such disulfide bonds stabilize the folded state of the HTH motif by primarily decreasing its unfolding rate (13).

Effect of the turn sequence on the folding thermodynamics and kinetics of PYY

For β-hairpins, it has been shown that the sequence of the reverse turn plays a critical role in both the stability and folding kinetics of the native fold (18,19). To explore the role of the turn in PYY folding, we further studied the folding thermodynamics and kinetics of two PYY mutants, S13A and P14A. The choice of these mutations is based on the study by Zerbe and co-workers which showed that both Ser13 and Pro14 are located in the turn region that links the C-terminal α-helix to the N-terminal polyproline helix and that the Ser13 to Ala mutation is especially disruptive to the native fold of PYY (11). Consistent with their NMR study, our CD results show that both mutations result in a decrease in the thermal stability of the PYY fold and that replacement of Ser13 with Ala is strongly destabilizing (Figure 3 and Table 1). This observation suggests that the native turn sequence in PYY is optimized for folding and is also in agreement with the finding of Hodges and Schepartz (5) that mutations in the turn region destabilize the folded state of a designed derivative of avian polypeptide (aPP), whose sequence and fold are similar to those of PYY.

The thermodynamic consequence of a mutation is a direct outcome of its effects on the folding and unfolding rates. For example, if a mutation preferentially destabilizes the folding transition state and the folded state, the folding rate of the mutant is expected to be slower than that of the wild-type, whereas the unfolding rate is largely unaffected. Thus, measurements of the folding kinetics of the mutant yield additional information that can be used to assess the characteristic of the transitions state (15). As shown (Figure 5), both mutations in the turn region perturb the relaxation rate of PYY, consistent with the equilibrium CD results. A mutation of the turn sequence may increase the chain entropy of the peptide and/or remove a native sidechain-sidechain or sidechain-backbone interaction. Thus, if the turn structure is formed (or becomes native-like) in the folding transition state, such a mutation would destabilize not only the native state but also the transition state, resulting in a decrease in the folding rate. As indicated (Table 2), at 30 °C the folding time of P14A is increased by about 146% from that of the wild-type, whereas the unfolding time is only increased by about 34%, suggesting that the transition state ensemble contains a native-like turn, which in the case of PYY, is stabilized by the conformational constraint on the backbone ϕ dihedral angle of Pro14. Further evidence supporting this notion comes from the folding time of S13A (Table 2), which also shows an appreciable increase from that of the wild-type (i.e., from 2.8 to 5.6 μs). In addition, the results obtained with S13A and P14A are consistent with the fact that the sequence of SPE is frequently found at the N-terminal end of α-helices in proteins as it is an efficient end-capping group and can increase the rate of α-helix formation (26). Furthermore, because the sidechain of Ser13 can form two hydrogen bonds with the main chain nitrogen and the sidechain of Glu16 (11), respectively, it is expected that elimination of these hydrogen bonds via mutation would result in not only a decrease in the folding rate but also an increase in the unfolding rate if only one of these hydrogen bonds is formed in the transition state, as observed (Table 2).

Effect of the hydrophobic cluster on the folding thermodynamics and kinetics of PYY

It is well known that the formation of a tightly packed hydrophobic cluster involving residues from both helices is essential to stabilize the folded hairpin structure (3-5,22).

However, kinetically this can be achieved by either increasing the folding rate or decreasing the unfolding rate. To dissect these possibilities, we studied the thermodynamic and kinetic effects of two mutations (i.e., Y21A and Y27A) that weaken the hydrophobic interactions between the two helices (11). As expected, both mutations destabilize the PP-fold (Figure 3 and Table 1), although the Y27A mutation has a much larger effect than the Y21A mutation, which is in agreement with the NMR measurements of Zerbe and co-workers (11).

As shown (Figure 5), mutation of either Y21 or Y27 to Ala results in a change in the *T*-jump induced relaxation time of the peptide. It is clear that at 30 °C this change mostly arises from a change in the unfolding time (Table 2). For example, the unfolding time of Y27A is 2.1 μs, which is significantly shorter than that (7.1 μs) of the wild-type, whereas its folding time only shows a marginal increase in comparison to that of the wild-type (i.e., from 2.8 to 4.3 μs). Thus, taken together, the results obtained with Y21A and Y27A suggest that the native hydrophobic cluster in PYY is formed at the downhill side of the folding free energy barrier.

Effect of temperature

The kinetic data obtained at 30 °C support a folding mechanism wherein the turn, but not the hydrophobic cluster, is formed in the transition state ensemble of PYY. To check whether such a conclusion remains true at higher temperatures, we further analyzed the folding and unfolding times of these PYY peptides at 50 °C. As shown (Table 3), the results of S13A and P14A corroborate the folding mechanism reached above. However, those of Y21A and Y27A seem to indicate that the hydrophobic cluster is partially formed in the transitions state, as their folding times are significantly longer than that of the wild-type. In other words, the kinetic data obtained at 50 °C suggest a folding mechanism of PYY that is different from that deduced from the 30 °C data. While it is possible that the characteristics of the transition state ensemble of PYY shows such a dependence on temperature, another possibility is that this apparent discrepancy arises from mutation-induced changes in the unfolded state. Many studies have shown that native and/or non-native hydrophobic contacts can exist in the denatured state of proteins (27-34). If such contacts exist in the thermally denatured state of wild-type PYY, they are expected to have a strong effect on the folding rate of the peptide. The NMR structure of PYY shows that Y21 and Y27 lie on the α-helix side, while their sidechains extend towards the PPII helix (Figure 1). Thus, it is possible that even in the unfolded state of PYY, interactions involving Y21 and Y27 and/or multiple residues on the PPII helix side persist. It is expected that such cross-strand interactions will reduce the entropic cost associated with the turn formation by effectively restricting the conformational space of the unfolded polypeptide chain, thus speeding up folding. In other words, mutations that eliminate or decrease such cross-strand interactions are expected to decrease the folding rate, as observed.

In addition, we investigated the folding kinetics of the A7Y mutant, which was previously shown to be more stable than the wild-type peptide (11). Our CD results confirm that the A7Y mutation increases the thermal stability of the PP fold (Figure 3 and Table 1). However, the stability increase is marginal and, as a result, the changes in the folding and unfolding rates induced by this mutation are close to the uncertainty of the experiments (Tables 2 and 3). To avoid over-interpretation of the experimental results, no further assessment is made.

Conclusions

In summary, we present a detailed mechanistic study of the folding mechanism of a naturally occurring helical hairpin (porcine PYY) that is free of disulfide bonds and other types of cross-links. At relatively low temperature (e.g., 30 °C) the effect of mutations in both the turn and hydrophobic cluster on the folding and unfolding rates of PYY supports a

folding mechanism in which the turn is formed in the transition state, whereas the hydrophobic cluster is consolidated on the downhill side of the folding free energy barrier. However, a more complex picture emerges at relatively higher temperatures (e.g., 50 °C) at which the folding rate of PYY is more significantly affected, even by mutations that weaken the cross-helix interactions. While this result could manifest a temperature dependent transition state ensemble, a more likely scenario is that it reflects changes in the unfolded conformational ensemble induced by such mutations. As the strength of hydrophobic interaction increases with increasing temperature, it is conceivable that the unfolded state ensemble of PYY is more compact at 50 °C than at 30 °C due to residual hydrophobic interactions between the two strands. Therefore, the comparatively slower folding rates of the hydrophobic deletion mutations at higher temperatures are reflections of their more flexible unfolded state ensembles, which allow the turn sequence to explore a larger region in the allowed conformational space, thus increasing the entropic penalty associated with turn formation and hence the folding time of the helical hairpin.

Acknowledgments

We gratefully acknowledge financial support from the National Institutes of Health (GM-065978 and RR-01348).

References

1. Huffman JL, Brennan RG. Prokaryotic transcription regulators: More than just the helix-turn-helix motif. Curr Opin Struct Biol. 2002; 12:98–106. [PubMed: 11839496]
2. Aravind L, Anantharaman V, Balaji S, Babu MM, Iyer LM. The many faces of the helix-turn-helix domain: Transcription regulation and beyond. FEMS Microbiol Rev. 2005; 29:231–262. [PubMed: 15808743]
3. Starovasnik MA, Braisted AC, Wells JA. Structural mimicry of a native protein by a minimized binding domain. Proc Natl Acad Sci USA. 1997; 94:10080–10085. [PubMed: 9294166]
4. Zondlo NJ, Schepartz A. Highly specific DNA recognition by a designed miniature protein. J Am Chem Soc. 1999; 121:6938–6939.
5. Hodges AM, Schepartz A. Engineering a monomeric miniature protein. J Am Chem Soc. 2007; 129:11024–11025. [PubMed: 17705497]
6. Wetlaufer DB. Nucleation, rapid folding, and globular intrachain regions in proteins. Proc Nat Acad Sci USA. 1973; 70:697–701. [PubMed: 4351801]
7. Kim PS, Baldwin RL. Specific intermediates in the folding reactions of small proteins and the mechanism of protein folding. Ann Rev Biochem. 1982; 51:459–8. [PubMed: 6287919]
8. Fersht AR. Nucleation mechanisms in protein folding. Curr Opin Struct Biol. 1997; 7:3–9. [PubMed: 9032066]
9. Religa TL, Johnson CM, Vu DM, Brewer SH, Dyer RB, Fersht AR. The helix-turn-helix motif as an ultrafast independently folding domain: The pathway of folding of Engrailed homeodomain. Proc Natl Acad Sci USA. 2007; 104:9272–9277. [PubMed: 17517666]
10. Woll MG, Gellman SH. Backbone thioester exchange: A new approach to evaluating higher order structural stability in polypeptides. J Am Chem Soc. 2004; 126:11172–11174. [PubMed: 15355097]
11. Neumoin A, Mares J, Lerch-Bader M, Bader R, Zerbe O. Probing the formation of stable tertiary structure in a model miniprotein at atomic resolution: Determinants of stability of a helical hairpin. J Am Chem Soc. 2007; 129:8811–8817. [PubMed: 17580866]
12. Amunson KE, Ackels L, Kubelka J. Site-specific unfolding thermodynamics of a helix-turn-helix protein. J Am Chem Soc. 2008; 130:8146–8147. [PubMed: 18529000]
13. Du D, Gai F. Understanding the folding mechanism of an α-helical hairpin. Biochemistry. 2006; 45:13131–13139. [PubMed: 17073435]
14. Dyer RB, Gai F, Woodruff WH, Gilmanshin R, Callender RH. Infrared studies of fast events in protein folding. Acc Chem Res. 1998; 31:709–716.

15. Fersht AR, Matouschek A, Serrano L. The folding of an enzyme, I. Theory of protein engineering analysis of stability and pathway of protein folding. J Mol Biol. 1992; 224:771–782. [PubMed: 1569556]

16. Keire DA, Kobayashi M, Solomon TE, Reeve JR Jr. Solution structure of monomeric peptide YY supports the functional significance of the PP-fold. Biochemistry. 2000; 39:9935–9942. [PubMed: 10933813]

17. Lerch M, Mayrhofer M, Zerbe O. Structural similarities of micelle-bound peptide YY (PYY) and neuropeptide Y (NPY) are related to their affinity profiles at the Y receptors. J Mol Biol. 2004; 339:1153–1168. [PubMed: 15178255]

18. Du D, Zhu Y, Huang CY, Gai F. Understanding the key factors that control the rate of β-hairpin folding. Proc Natl Acad Sci USA. 2004; 101:15915–15920. [PubMed: 15520391]

19. Du D, Tucker MJ, Gai F. Understanding the mechanism of β-hairpin folding via ϕ-value analysis. Biochemistry. 2006; 45:2668–2678. [PubMed: 16489760]

20. Zhu Y, Fu X, Wang T, Tamura A, Takada S, Saven JG, Gai F. Guiding the search for a protein's maximum rate of folding. Chem Phys. 2004; 307:99–109.

21. Huang CY, Getahun Z, Zhu Y, Klemke JW, DeGrado WF, Gai F. Helix formation via conformational diffusion search. Proc Natl Acad Sci USA. 2002; 99:2788–2793. [PubMed: 11867741]

22. Fezoui Y, Weaver DL, Osterhout JJ. De novo design and structural characterization of an α-helical hairpin peptide: A model system for the study of protein folding intermediates. Proc Natl Acad Sci USA. 1994; 91:3675–3679. [PubMed: 8170968]

23. Williams S, Causgrove TP, Gilmanshin R, Fang KS, Callender RH, Woodruff WH, Dyer RB. Fast events in protein folding: Helix melting and formation in a small peptide. Biochemistry. 1996; 35:691–697. [PubMed: 8547249]

24. Walsh STR, Cheng RP, Wright WW, Alonso DOV, Daggett V, Vanderkooi JM, DeGrado WF. The hydration of amides in helices; a comprehensive picture from molecular dynamics, IR, and NMR. Protein Sci. 2003; 12:520–531. [PubMed: 12592022]

25. Mukherjee S, Chowdhury P, Gai F. Infrared study of the effect of hydration on the amide I band and aggregation properties of helical peptides. J Phys Chem B. 2007; 111:4596–4602. [PubMed: 17419612]

26. Wang T, Zhu Y, Getahun Z, Du D, Huang CY, DeGrado WF, Gai F. Length-dependent helix-coil transition kinetics of nine alanine-based peptides. J Phys Chem B. 2004; 108:15301–15310.

27. Neri D, Billeter M, Wider G, Wüthrich K. NMR determination of residual structure in a urea-denatured protein, the 434-repressor. Science. 1992; 257:1559–1563. [PubMed: 1523410]

28. Wilson G, Hecht L, Barron LD. Residual structure in unfolded proteins revealed by Raman optical activity. Biochemistry. 1996; 35:12518–12525. [PubMed: 8823188]

29. Mok YK, Kay CM, Kay LE, Forman-Kay J. NOE data demonstrating a compact unfolded state for an SH3 domain under non-denaturing conditions. J Mol Biol. 1999; 289:619–638. [PubMed: 10356333]

30. Tang Y, Rigotti DJ, Fairman R, Raleigh DP. Peptide models provide evidence for significant structure in the denatured state of a rapidly folding protein: The villin headpiece subdomain. Biochemistry. 2004; 43:3264–3272. [PubMed: 15023077]

31. Tucker MJ, Oyola R, Gai F. Conformational distribution of a 14-residue peptide in solution: A fluorescence resonance energy transfer study. J Phys Chem B. 2005; 109:4788–4795. [PubMed: 16851563]

32. Mok KH, Kuhn LT, Goez M, Day IJ, Lin JC, Andersen NH, Hore PJ. A pre-existing hydrophobic collapse in the unfolded state of an ultrafast folding protein. Nature. 2007; 447:106–110. [PubMed: 17429353]

33. Zhou R, Eleftheriou M, Royyuru AK, Berne BJ. Destruction of long-range interactions by a single mutation in lysozyme. Proc Natl Acad Sci USA. 2007; 104:5824–5829. [PubMed: 17389393]

34. Das P, King JA, Zhou R. β-strand interactions at the domain interface critical for the stability of human lens γ-crystallin. Protein Sci. 2010; 19:131–140. [PubMed: 19937657]

Abbreviations used

CD	circular dichroism
IR	infrared
***T*-jump**	temperature-jump
HTH	helix-turn-helix motif

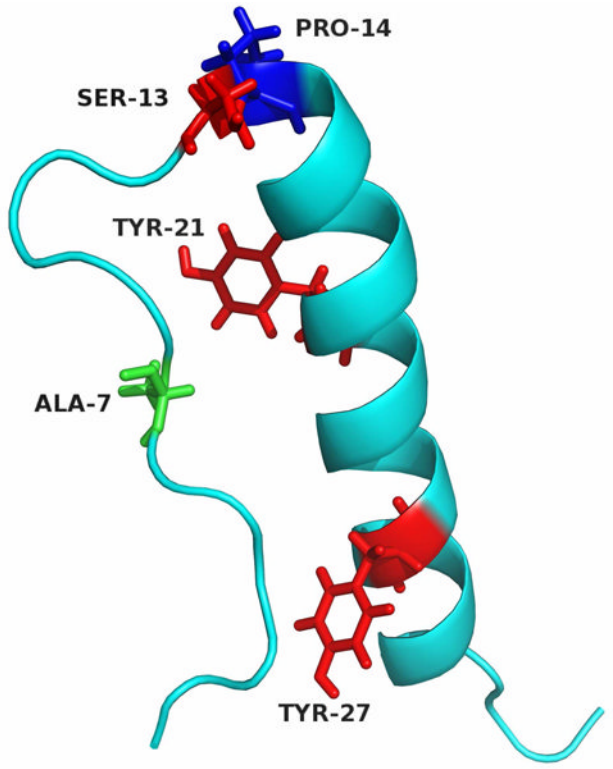

Figure 1.
NMR structure of porcine PYY (PDB code: 2RLK). The side chains of those residues targeted for mutation are shown in stick representation.

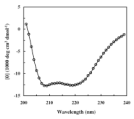

Figure 2.
Far-UV CD spectrum of PYY at 25 °C.

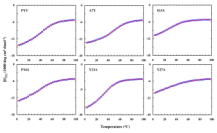

Figure 3.
Thermal unfolding CD curves of PYY and its mutants, as indicated. Lines are fits to the two-state model described in the text.

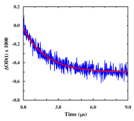

Figure 4.
A representative relaxation kinetic trace of PYY in response to a *T*-jump of 9.2 °C, from 23.0 to 32.2 °C. For clarity, an unresolved kinetic phase has been subtracted from these data. The smooth line represents the best fit of these data to a single-exponential function with a life time of 1.9 μs.

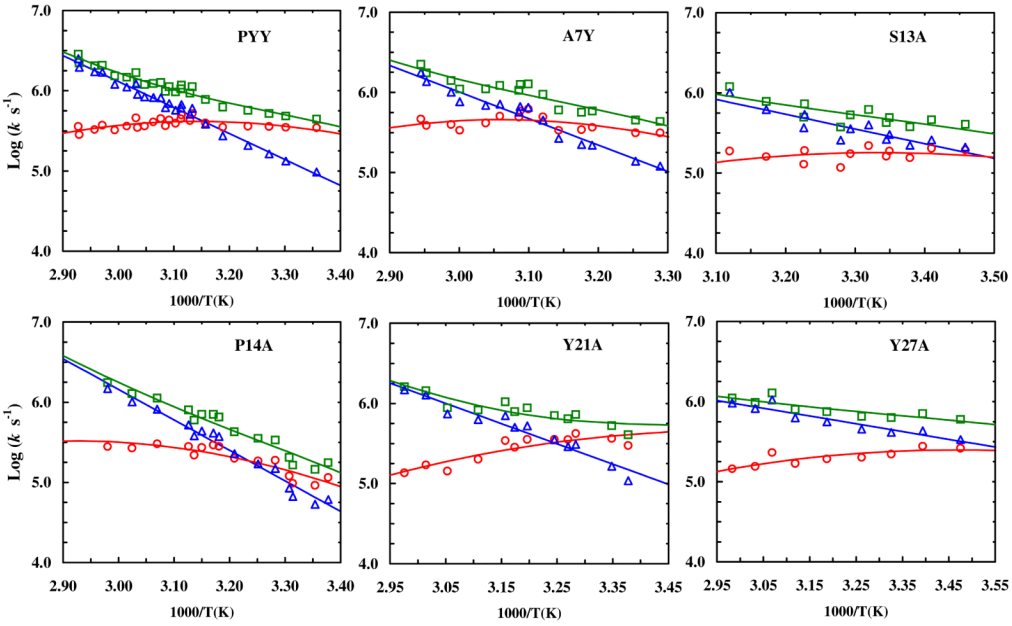

Figure 5.

Arrhenius plots of the observed relaxation rates (□) as well as folding (○) and unfolding (△) rate constants for the peptides as indicated in the respective panels. For each peptide, lines represent global fits of the folding and unfolding rate constants to the Eyring equation, $\ln(k) = \ln(D) - \Delta G^{\neq}/(RT)$, where D is a constant and $\Delta G^{\neq}$ is the free energy of activation. In this work, D was arbitrarily set as 10^{10} s^{-1} and $\Delta G_f^{\neq}$and $\Delta G_u^{\neq}$ were constrained so that $\Delta G_f^{\neq}(T) - \Delta G_u^{\neq}(T) = \Delta G^0(T)$, where $\Delta G^0(T)$ is the equilibrium free energy of unfolding at temperature T.

Table 1

Unfolding thermodynamic parameters of PYY and mutants obtained from global fitting of their CD thermal melting curves.

Peptide	ΔH^0_m (kcal mol^{-1})	ΔS^0_m (cal K^{-1} mol^{-1})	ΔC_p (cal K^{-1} mol^{-1})	T_m (°C)
PYY	14.5 ± 1.6	45.8 ± 4.8	221 ± 25	44.0 ± 1.6
A7Y	13.5 ± 1.3	41.9 ± 3.9	333 ± 47	48.7 ± 2.0
S13A	5.5 ± 0.7	19.1 ± 2.5	221 ± 25	13.5 ± 2.0
P14A	10.2 ± 0.7	33.1 ± 2.1	221 ± 25	36.0 ± 1.9
Y21A	15.8 ± 0.2	51.4 ± 0.7	139 ± 41	35.1 ± 0.9
Y27A	3.3 ± 0.5	11.8 ± 1.9	100 ± 29	4.1 ± 2.7

Table 2

Folding and unfolding rate constants of PYY and mutants at 30 °C.

Peptide	k_f^{-1} (μs)	k_u^{-1} (μs)
PYY	2.8 ± 0.5	7.1 ± 1.3
A7Y	3.5 ± 0.6	9.6 ± 1.7
S13A	5.6 ± 1.0	2.8 ± 0.5
P14A	6.9 ± 1.2	9.5 ± 1.7
Y21A	2.8 ± 0.5	4.2 ± 0.8
Y27A	4.3 ± 0.8	2.1 ± 0.4

Table 3

Folding and unfolding rate constants of PYY and mutants at 50 °C.

Peptide	k_f^{-1} (μs)	k_u^{-1} (μs)
PYY	2.4 ± 0.4	1.6 ± 0.3
A7Y	2.2 ± 0.4	2.0 ± 0.4
S13A	7.5 ± 1.4	1.2 ± 0.2
P14A	3.6 ± 0.6	1.6 ± 0.3
Y21A	4.6 ± 0.8	1.3 ± 0.3
Y27A	5.5 ± 1.0	1.3 ± 0.2